American Mineralogist, Volume 82, pages 571–581, 1997

Molar volumes of mixing of almandine-pyrope and almandine-spessartine garnets and the crystal chemistry and thermodynamic-mixing properties of the aluminosilicate garnets

CHARLES A. GEIGER[1] AND ANNE FEENSTRA[2]*

[1]Mineralogisch-Petrographisches Institut, Christian-Albrechts-Universität zu Kiel, Olshausenstr. 40, D-24098 Kiel, Germany
[2]Mineralogisch-Petrographisches Institut, Universität Bern, Baltzer-Strasse 1, CH-3012 Bern, Switzerland

ABSTRACT

The aluminosilicate garnet binaries almandine-pyrope and almandine-spessartine were studied by powder X-ray and ^{57}Fe Mössbauer methods. Refinements of the unit-cell constants along the almandine-pyrope join show that the volumes of mixing are ideal. Those of the almandine-spessartine join show very small positive deviations from ideality, which can be fitted with a symmetric model having an interaction parameter of $W^V = 0.24$ (± 0.05) cm^3/mol. Mössbauer spectra recorded at 298 and 77 K show the presence of small amounts of $^{[6]}Fe^{3+}$, which in the case of almandine-pyrope garnets is also measurable from microprobe analyses. The amount of Fe^{3+} is generally less than 3.5% of the total Fe for the almandine-pyrope garnets and 1–2% for almandine-spessartine garnets. The molar volumes of mixing of the aluminosilicate garnet binaries are interpreted using a crystal-chemical model involving rigid tetrahedral rotation. The degree of tetrahedral rotation is not linear with increasing size of the divalent X-site cation for the four common aluminosilicate garnet end-members or along the solid solution binary pyrope-grossular. The vibrational entropies of mixing should be positively correlated with the volumes of mixing in the case of garnet, but the masses of the X-site cations must also be considered. The phonon density of states at low energies should show the vibrations of the weakly bonded divalent cations and rigid-unit modes related to tetrahedral rotation. Positive excess vibrational entropies of mixing along a binary could result from increased amplitudes and lower frequencies of vibration of the smaller of the two X-site cations substituting within larger and more distorted dodecahedral sites, as compared to the X site in the smaller volume end-member.

INTRODUCTION

Aluminosilicate garnet solid solutions found in metapelites, amphibolites, and granulites can largely be described using four end-member components within the system $Fe_3Al_2Si_3O_{12}$(almandine)-$Mn_3Al_2Si_3O_{12}$ (spessartine)-$Mg_3Al_2Si_3O_{12}$(pyrope)-$Ca_3Al_2Si_3O_{12}$(grossular). For thermodynamic calculations in such compositionally complex systems, it is advantageous to clarify the simpler binary mixing properties first and to extrapolate, with the use of solution models, into more compositionally complicated multicomponent systems. Of the thermodynamic functions, the volumes of mixing are relevant in petrological calculations because they enter into the Gibbs free energy with increasing importance with increasing pressure. They are also important because they can be determined, as compared to the entropies and enthalpies of mixing, very precisely and accurately. Therefore, the volumes of mixing can yield valuable information about the thermodynamic mixing properties as well as structural changes accompanying changes in composition along a solid solution.

We present herein, molar volumes of mixing for two aluminosilicate garnet binaries, namely almandine-pyrope and almandine-spessartine. Molar volumes of mixing for the former have already been given (Geiger et al. 1987), but were remeasured and reinterpreted using more precise and better X-ray powder data. The molar volumes of mixing for the almandine-spessartine join were determined quantitatively for the first time. In addition, ^{57}Fe Mössbauer spectra were collected on garnets from both binaries at 293 and 77 K to determine the amount of Fe^{3+} present in nominally Fe^{3+}-free aluminosilicate garnet solid solutions.

The volumes of mixing, resulting from the substitution of different cations within the dodecahedral X site, are interpreted using a crystal-chemical model involving rigid tetrahedral rotation. In addition, the possible vibrational entropies of mixing are considered in lieu of the volumes of mixing and the crystal chemistry of garnet.

EXPERIMENTAL METHODS

Synthesis

The almandine-pyrope garnets studied herein are the same materials described in Geiger et al. (1987) and Geiger et al. (1989).

* Present address: Institut für Petrologie, Geozentrum, Universität Wien, Althanstrasse 14, A-1090 Vienna, Austria.

TABLE 1. Synthesis conditions, compositions, unit-cell constants, and molar volumes of almandine-spessartine garnets

Run no.	P (kbar)	T (°C)	Duration (days)	Mn/(Mn + Fe)		a_0 (Å)†	Molar volume (cm³)
				Intended	Measured*		
AL100F	20	950	7	0.000	0.000	11.5283(6)	115.341(18)
AL100G	20	925	5	0.000	0.000	11.5270(7)	115.302(21)
S5	20	950	6	0.050	0.081(11)	11.5369(12)	115.599(36)
S10	20	920	8	0.100	0.100(19)	11.5366(8)	115.590(24)
S12l	20	950	5	0.125	0.149(10)	11.5389(5)	115.660(15)
S12l2	20	925	5	0.125	0.127(8)	11.5405(4)	115.708(12)
S12L2	20	925	5	0.125	0.120(8)	11.5383(3)	115.642(9)
S25/2	20	980	5	0.250	0.254(9)	11.5523(3)	116.063(9)
S25l	20	970	3	0.250	0.251(26)	11.5509(3)	116.021(9)
S25l2	20	970	5	0.250	0.247(13)	11.5504(2)	116.006(6)
S25K	20	970	5	0.250	0.251(13)	11.5502(4)	116.000(12)
S50F	20	1000	5.5	0.500	0.519(11)	11.5745(3)	116.733(9)
S50l	20	1000	4	0.500	0.509(10)	11.5736(2)	116.706(6)
S50l2	20	1000	5	0.500	0.514(13)	11.5753(4)	116.758(12)
S50J	20	1000	5	0.500	0.543(15)	11.5757(2)	116.770(6)
S62C	20	1000	4	0.625	0.709(18)	11.5906(9)	117.221(27)
S62C1	20	1000	5	0.625	0.726(19)	11.5918(2)	117.258(6)
S75C	20	1000	7	0.750	0.826(7)	11.6025(6)	117.583(18)
S75K	20	1000	3	0.750	0.785 (20)	11.5967(3)	117.406(9)
S75M	20	1000	5	0.750	0.798(13)	11.6003(4)	117.516(12)
S87.5C	20	1000	3	0.875	0.915(10)	11.6102(5)	117.817(15)
SP100(15)	20	980	5	1.000	1.000	11.6139(3)	117.930(9)
SP100(16)	20	980	6	1.000	1.000	11.6151(6)	117.966(18)

Note: Numbers in parentheses represent one standard deviation expressed in terms of last digit(s).
* Measured compositions are based on at least 18 spot analyses.
† a_0 is based on 14–24 reflections.

Almandine-spessartine garnets were prepared in two steps following the procedure outlined by Bohlen et al. (1983). First, glasses of stoichiometric garnet compositions were prepared by melting specpure oxide mixes of MnO_2, Fe_2O_3, Al_2O_3, and SiO_2 in thick-walled graphite crucibles with tight-fitting lids at temperatures between 1370–1425 °C. To avoid oxidation of the graphite crucible, the oven was purged with Ar gas. Reduction times in the melt were such that the crucible was removed from the oven and quenched on a thick steel plate just before iron metal saturation. A glass was considered optimal if it was greenish for the almandine-rich compositions and nearly colorless for those glasses richer in a spessartine component.

Glasses of the proper color were finely ground, tightly packed in graphite capsules (~300 mg), and heated in a piston-cylinder device at 920–1000 °C and 20 kbar for 3–8 d. A total of more than 25 Al-Sp garnet syntheses were conducted, as the garnets were used as starting materials for Fe-Mn exchange experiments with ilmenite (Feenstra and Engi, unpublished manuscript). Table 1 lists the synthesis conditions.

Electron microprobe analysis

Pyrope-almandine garnets were reanalyzed using wavelength-dispersive (WDS) techniques at the CAU-Kiel using a Cameca microprobe. For each garnet composition, one small polycrystalline chip was taken from the center of the experimental charge and one from the rim, which was in contact with the graphite capsule, and mounted in an epoxy holder and polished. The operating conditions were 15 kV accelerating potential with a 15 nA beam current and a beam size of 1–2 μm. Peak counting times were 20 s for Al, Si, Fe, Mg, Mn, and Ca and 10 s for the backgrounds. Wollastonite, iron metal, Al_2O_3, and MgO were used as standards, and the raw data were corrected with the PAP procedure.

Almandine-spessartine garnets were measured in Bern also using WDS analysis. Operating conditions were a 15 kV accelerating potential, 20 nA beam current, and a beam diameter of 1–2 μm. Counting times of 30 s were used for Fe, Mn, Al, and Si. Backgrounds were measured for 10 s. Standards used included synthetic ilmenite (Fe), pyrophanite (Mn), spessartine (Mn, Al, Si), almandine (Fe, Si, Al), and natural garnet (Si, Al). Full ZAF corrections were made to the spectrometer data. The quality and reproducibility of the analyses were monitored by measuring well-known standards (Fe- and Mn-containing ilmenite, garnets, fayalite, and tephroite) in the sessions during which the synthetic garnets were analyzed.

^{57}Fe Mössbauer spectroscopy

All synthetic Al-Py and five Al-Sp garnet solid-solution compositions were measured at 293 and 77 K with a nominal 50 mC ^{57}Co-Rh source. Ground garnet powders were pressed together with cornstarch into pellets of diameter 12.0 mm with approximately 5 mg Fe^{2+}/cm^2. Mirror image spectra were collected on a 512 multichannel analyzer and then folded. The spectra were fitted with the program MÖSALZ (courtesy of W. Lottermoser, Salzburg University) using single Lorentzian lines for the Fe^{2+} doublet (Geiger et al. 1992). The low-temperature measurements were made with an Oxford cryostat with the absorber held at approximately 77 K. The lower temperature

measurements give a better estimate of the Fe^{2+}/Fe^{3+} ratios because of the differences in the recoil-free fraction of Fe in both sites. Three spectra, one on end-member almandine, and one solid-solution composition from the Al-Py and Al-Sp solid-solution joins are shown in Figure 1a, b, and c. The hyperfine parameters for the Al-Py garnets are given in Geiger et al. (1990) and those for Al-Sp garnets in Geiger (1993). They show only slight differences as a function of composition.

Unit-cell refinements and Rietveld refinements

Powder X-ray data on the spessartine-almandine garnets were collected up to ~130° 2θ on a Philips diffractometer using Cu*K*α radiation. Background noise was minimized by using single-crystal corundum sample holders. The slow-scan (0.5° 2θ/min) diffraction data were corrected for instrumental shift using metallic Si as an internal standard. Garnet unit-cell edges were calculated by weighted least-squares regression of 14–24 reflections using the program GITTER (Hummel 1988). Results are listed in Table 1.

The unit-cell constants of two different end-member almandine and pyrope samples from the almandine-pyrope series were determined using a Siemens D-5000 diffractometer using Cu*K*α radiation. Diffractograms were recorded between 15 and 160° 2θ in 0.01° steps with 4 s counting time per degree. National Bureau of Standards Si (640b) was used as an internal standard and least-squares regressions were made using the program Pulver-92.

Eight Al-Py garnet solid solutions were ground manually under acetone using a boron nitride mortar and pestle and mounted as thin slurries dispersed with acetone on a single-crystal quartz plate (i.e., zero-background holder) for Rietveld refinements. Step-scan XRD data were collected using a SCINTAG automated diffractometer system, with a horizontal goniometer (22 cm radius) equipped with a solid-state Ge detector. Detector dead-time corrections were applied automatically during data collection. Soller slits were used in both the incident and diffracted beam paths. A complete description of the samples and details of XRD data collection procedure are given in Table 2.

The least-squares structure refinements were conducted with a modified version of the Rietveld-analysis program

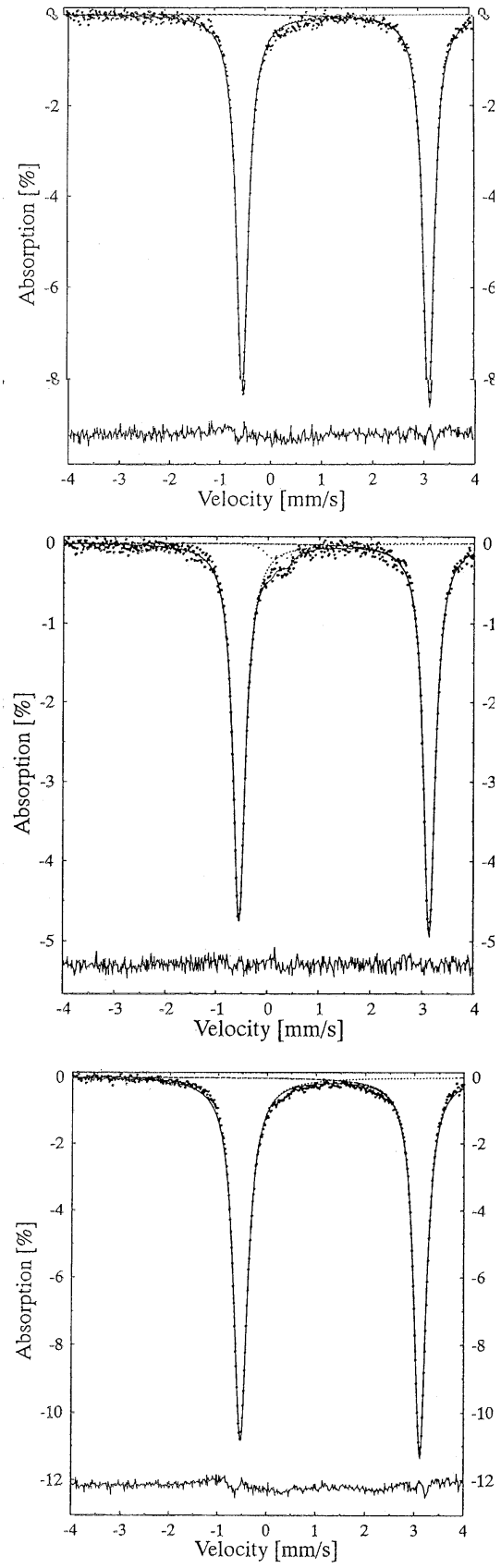

→

FIGURE 1. (**a**) The ^{57}Fe Mössbauer spectrum of end-member almandine from the pyrope-almandine binary recorded at 77 K. (**b**) The ^{57}Fe Mössbauer spectrum of garnet $Al_{61}Py_{39}$ recorded at 77 K showing a small Fe^{3+} doublet with an area of 3.4% of the total Fe. (**c**) The ^{57}Fe Mössbauer spectrum of $Al_{21.5}Sp_{78.5}$ recorded at 77 K. The presence of $^{[6]}Fe^{3+}$ in these garnets is confirmed by the small shoulder present on the high-energy wing of the low-velocity Fe^{2+} line. It is only fitted in the case of the $Al_{61}Py_{39}$ garnet. The Fe^{2+} doublet was fitted using two independent Lorentzian lines.

TABLE 2. Sample and XRD data collection information for almandine-pyrope garnets

Formula	$(Fe^{2+}_x Mg_{1-x})Al_2(SiO_4)_3$
Space group	$Ia\bar{3}d$
Sample mass (mg)	10–25
Particle size	<400 mesh (38 μm)
Radiation wavelengths	
Cu$K\alpha_1$ (Å)	1.54059
Cu$K\alpha_2$ (Å)	1.54433
$I(K\alpha 2)/I(K\alpha 1)$	0.5
XRD operating conditions	45 kV, 40 mA
	2 mm (~0.52°) divergence slit
	0.3 mm (0.07°) receiving slit
Absorption coefficients (cm^{-1})	94 ($x = 0$) to 524 ($x = 1$)
2θ scan range (deg.)	15–162
Step width (deg.)	0.12
Number of steps in full pattern	1225
Step counting time (s)	2
Total counting time (min)	48
Maximum step intensity (counts)	4500
Average background (counts)	10–40
Number of unique Bragg reflections	143
Number of structural parameters	9
Number of profile parameters	14

DBW3.2 (Hill 1985; Wiles and Young 1981). A minor corundum impurity was identified in several of the samples, most notably in $Al_{75}Py_{25}$ (<5 vol%). The corundum peaks, which are usually located near the shoulders of the most intense garnet reflections, were probably not the result of contamination during XRD preparation. An additional nongarnet impurity phase (<5 vol%) observed in $Al_{93}Py_{07}$ could not be identified. Refinement was continued until the parameter shifts in the last cycle were less than one-quarter of their associated estimated standard deviations. Calculated and difference profiles for a representative refinement are shown in Figure 2.

In this manuscript only the results from the unit-cell determinations are presented (Table 3).

RESULTS

The Al-Py garnets have been described previously (Geiger et al. 1987; Geiger et al. 1989). The present powder X-ray measurements represent an improvement over those given previously. The measurements made on the solid-solution compositions with the SCINTAG device were superior because the more sensitive Ge detector obtains better signal-to-background ratios. These measurements showed that in a few samples small amounts of corundum were present, which were not detected by Geiger et al. (1987). In addition, the present WDS probe results gave bulk compositions slightly richer in Fe than the older EDS analyses and that are in good agreement with the intended synthetic compositions (Table 4). Garnet structural formulas were calculated assuming eight cations and 12 O atoms per formula unit. Stoichiometric constraints require small amounts of Fe^{3+} for most samples, which was assigned to the octahedral sites (Table 4). This is consistent with the very small amounts of corundum observed in a few samples. The unit-cell refinements made with the Siemens diffractometer on two different almandine syntheses gave cell dimensions of 11.5290(3) Å and 11.5293(4) Å. These values are slightly larger than those presented in Geiger et al. (1987).

The Al-Sp syntheses yielded >99% garnet of fairly homogeneous composition. Very small amounts of quartz, corundum, or spinel were detected in some syntheses, particularly by using backscattered electron-imaging methods with the electron microprobe. A few garnets showed relatively large variations in X_{Mn} from the nominal compositions (Table 1). End-member almandine synthesized in Bern, using two different starting glasses, gave unit-cell dimensions of 11.5270(7) and 11.5283(6) Å. Spessartine was also synthesized in two different experiments giving unit-cell dimensions of 11.6139(3) and 11.6151(6) Å (Table 1).

The electron microprobe results of the Al-Sp garnets show small deviations from the intended starting compositions with most garnets slightly too high in X_{Mn} (Table 1). As the deviation tends to increase with increasing X_{Mn}, and because several syntheses contain small amounts of corundum, quartz, or both, the trend could possibly be explained by preferential loss of some Fe to the graphite crucibles during the melting procedure. Unlike the Al-Py garnets, structural formulas calculated from the microprobe data do not provide evidence for the presence of Fe^{3+}. As demonstrated in Table 5 for those garnets examined by Mössbauer spectroscopy, they are very close to $(Fe,Mn)_3Al_2Si_3O_{12}$ compositions.

Mössbauer spectra show that small amounts of $^{[6]}Fe^{3+}$ are present in both garnet solid solutions (Fig. 1) with slightly more in the Al-Py than in the Al-Sp garnets. The small amounts of Fe^{3+}, the strong overlap of the doublets, and the uncertainties regarding the differences in the recoil-free fractions of Fe^{2+} and Fe^{3+} in garnet make it difficult to quantify the exact amount of $^{[6]}Fe^{3+}$. In the case of the Al-Py garnets it is less than 3.5% of the total Fe and for the Al-Sp garnets less than 1–2%. The spectra do demonstrate, though, that most synthetic almandine and almandine-containing aluminosilicate garnet solid solutions contain some $^{[6]}Fe^{3+}$ (Geiger et al. 1988).

The molar volumes of mixing for almandine-pyrope and almandine-spessartine solid solutions are shown in Figures 3 and 4, respectively. Deviations from ideal thermodynamic mixing are small to nonexistent. The data for the almandine-pyrope binary were analyzed using two different least-squares fitting procedures considering the errors in both composition and in molar volume. The first method was that of Berkson (1950) and the second was described in Deming (1964). Both gave essentially the same results. The method of Berkson is adopted here and shows that the data are best fitted by a linear function in which the molar volumes are described by

$$V(\text{cm}^3/\text{mol}) = 115.338\ (\pm 0.011) - 2.195\ (\pm 0.019) X_{Py} \quad (1)$$

where X_{Py} is the mole fraction of pyrope in the garnet. The introduction of higher order terms in a quadratic polynomial were shown not to be statistically significant by use of F-tests. The molar volumes of mixing for the

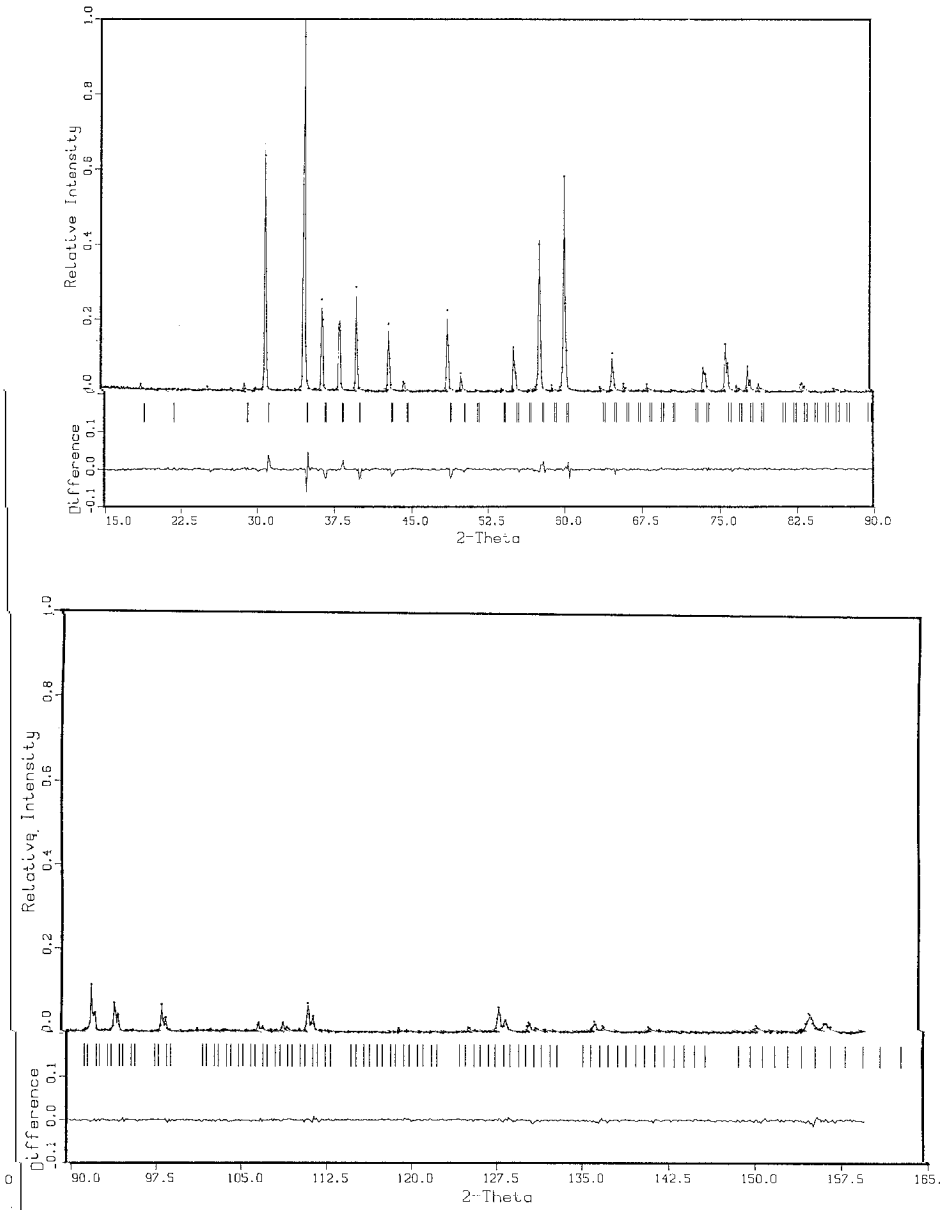

FIGURE 2. Observed (solid points), calculated (best-fit line) and difference plot for garnet of composition $Py_{75}Al_{25}$. The positions of all allowed Bragg reflections are indicated as vertical lines directly beneath the profile. The background has been fitted by a fourth-order polynomial.

almandine-spessartine binary show considerably more scatter. Most of the data show a slight positive deviation from ideality and hence the data were fitted with the most simple nonlinear polynomial (i.e., quadratic equation) giving

$$V(\text{cm}^3/\text{mol}) = 115.33\ (\pm 0.01) + 2.69\ (\pm 0.03)X_{Sp} - 0.24(\pm 0.05)X_{Sp}^2 \quad (2)$$

where X_{Sp} is the mole fraction of spessartine in the garnet. The excess molar volumes can be fitted with a symmetric Margules mixing model where (Thompson 1967)

$$\Delta V^{XS} = X_1 X_2 W^V \quad (3)$$

with $W^V = 0.24\ (\pm 0.05)$ cm³/mol.

DISCUSSION

Molar volumes

The molar volumes of the almandine-pyrope garnets (Table 3) are in reasonable agreement with those presented earlier (Geiger et al. 1987). The more recent results are preferred because of the better X-ray technique used and the advantages of the Rietveld method. In ad-

TABLE 3. Compositions, unit-cell constants and molar volumes of almandine-pyrope garnets

Intended composition	Mole fraction Mg/(Mg + Fe^{2+})*	a_0 (Å)†	a_0 (Å)	Molar volume (cm^3)
Al_{100}		11.525(1)	11.5291(3)‡	115.358(9)
$Al_{93}Py_{07}$	0.071(1)	11.521(1)	11.5227(2)	115.166(6)
$Al_{85}Py_{15}$	0.154(5)	11.515(1)	11.5170(2)	114.995(6)
$Al_{75}Py_{25}$	0.259(30)	11.508(1)	11.5105(2)	114.800(6)
$Al_{60}Py_{40}$	0.393(30)	11.498(1)	11.4995(2)	114.472(6)
$Al_{50}Py_{50}$	0.493(8)	11.492(1)	11.4925(3)	114.263(9)
$Al_{38}Py_{62}$	0.614(18)	11.480(1)	11.4830(2)	113.979(6)
$Al_{25}Py_{75}$	0.752(23)	11.472(1)	11.4737(2)	113.703(6)
$Al_{10}Py_{90}$	0.910(18)	11.462(1)	11.4612(2)	113.332(6)
Py_{100}		11.454(1)	11.4555(3)‡	113.163(9)

* Numbers in parentheses represent one standard deviation expressed in terms of the last digit(s).
† Geiger et al. (1987).
‡ Powder refinement with Siemens diffractometer.

dition, the compositions of the samples were determined better with the more accurate WDS microprobe results, which are also in better agreement with the intended starting compositions in comparison with the previous EDS analyses. The latter showed slight deviations toward more pyrope-rich bulk compositions. The unit-cell measurements on the solid solutions indicate ideal volumes of mixing across the Al-Py join. The molar volumes of Al-Sp garnets show, with the exception of one datum, very small positive deviations from ideal behavior. The molar volumes of four almandine-spessartine solid solutions presented by Hsu (1968) plot slightly below our values and show no measurable deviations from ideal mixing.

Recent IR and Mössbauer spectroscopic studies indicate that the molar volumes of the aluminosilicate garnets are increased slightly by the presence of $^{[6]}Fe^{3+}$ and $(O_4H_4)^{4-}$ groups substituting for SiO_4^{4-} tetrahedra in the hydrogarnet substitution. These substitutions are indeed limited, but both increase the volume over a $^{[6]}Fe^{3+}$- and OH^--free composition (Geiger et al. 1988; Geiger et al. 1991). These ''extra components'' are believed responsible for much of the variation observed in the literature for the unit-cell dimension of almandine. The values presented here for almandine are in reasonable agreement with unit-cell parameters recorded in other studies (Hsu 1968; Cressey et al. 1978; Geiger et al. 1987). The optimal value for end-member stoichiometric almandine, for which synthesis may not be possible using the present methods, is considered to be 11.525(2) Å (Geiger et al. 1988). Anovitz et al. (1993) synthesized almandine in a similar way to that used here, but measured a smaller unit-cell edge of 11.521(1) Å.

The measured unit-cell dimensions of spessartine of 11.6139(3) and 11.6151(6) Å (Table 1) are in good agreement with previous studies (Mottana 1974; Hsu 1968; Koziol 1990; Geiger and Armbruster 1997). Small differences between different published unit-cell dimensions could be related to the presence of $^{[6]}Mn^{3+}$ and OH^-.

In this analysis of the ΔV^{mix} the latter substitution was ignored, because for garnets synthesized anhydrously from glass the OH^- substitution is not relevant. The effects of $^{[6]}Fe^{3+}$ and $^{[6]}Mn^{3+}$ were also not evaluated, considering the small amounts present. It should be stated, however, that with present-day X-ray powder diffractometers and fitting methods and the precision now attainable in unit-cell determinations the presence of defects and small additional components must be addressed more carefully. These small, but measurable, contributions to the unit-cell dimension of garnet, combined with the differences in experimental synthesis methods adopted in different laboratories, render further quantitative evaluations and comparisons of various molar volume determinations of the garnet end-members questionable.

Crystal chemistry and molar volumes of mixing

The static crystal chemistry of the garnet structure and its response to changing X-site chemistry has been well documented (Menzer 1928; Zemann 1962; Born and Zemann 1964; Novak and Gibbs 1971; Meagher 1980; Merli et al. 1995). Recent temperature-dependent single-crystal X-ray refinements of synthetic end-member silicate garnets permit a better understanding of the dynamic structural properties (Geiger et al. 1992; Armbruster et al. 1992; Armbruster and Geiger 1993; Geiger and Armbruster 1997). These studies confirm the static-based interpretation that rigid corner-sharing tetrahedra and octahedra can be considered as forming an $\{^{[6]}Al_2(SiO_4)_3\}^{6-}$ framework (Zemann 1962), because they show that both polyhedra, unlike the dodecahedra, vibrate as rigid bodies (at least between 100 and 500 K). The divalent and more weakly bonded X-site cations occupy the large dodecahedral cavities, where they vibrate in a strongly anisotropic manner (Armbruster and Geiger 1993).

The substitution of different divalent cations in the

TABLE 4. Structural formulas of almandine-pyrope garnets

Sample	Al_{100}	$Al_{93}Py_{07}$	$Al_{85}Py_{15}$	$Al_{75}Py_{25}$	$Al_{60}Py_{40}$	$Al_{50}Py_{50}$	$Al_{38}Py_{62}$	$Al_{25}Py_{75}$	$Al_{10}Py_{90}$	Py_{100}
Si	2.99	3.01	2.99	2.99	3.03	3.00	3.01	3.00	3.01	3.02
Al	1.97	1.98	1.98	1.98	1.97	1.96	1.97	1.98	1.98	1.98
Fe^{3+}	0.03	0.01	0.04	0.03	0.00	0.05	0.01	0.02	0.01	0.00
Fe^{2+}	2.99	2.80	2.53	2.22	1.81	1.52	1.17	0.74	0.27	0.00
Mg	0.00	0.21	0.46	0.78	1.18	1.48	1.84	2.26	2.74	2.99
Mg/(Mg + Fe^{2+})	0.00	0.07	0.15	0.26	0.39	0.49	0.61	0.75	0.91	1.00

Note: Formulas are based on 12 O atoms and 8 cations. All samples, except pryope, were studied by Mössbauer spectroscopy.

TABLE 5. Structural formulas of almandine-spessartine garnets

Sample number	Al100F	S12I2	S25K	S50I	S75K	S87.5C	SP100(15)
Si	2.98(3)*	2.99(2)	2.99(2)	3.01(1)	3.01(2)	2.97(3)	3.00(3)
Al	2.02(4)	2.00(3)	1.99(2)	1.99(1)	2.01(2)	2.02(3)	2.00(3)
Fe^{2+}	3.01(3)	2.63(4)	2.27(4)	1.47(3)	0.64(6)	0.26(3)	3.00(3)
Mn	0.00	0.38(2)	0.76(4)	1.53(3)	2.33(6)	2.77(5)	0.00
$Mn/(Mn + Fe^{2+})$	0.00	0.127(8)	0.251(13)	0.509(10)	0.785(20)	0.915(10)	1.000

Note: Formulas are based on 12 O atoms. Intermediate garnets were studied by Mössbauer spectroscopy.
* Numbers in parentheses represent one standard deviation expressed in terms of last digit(s).

X-site and their effect on the garnet framework can be interpreted using a model based on rigid tetrahedral rotation (Born and Zemann 1964). A tetrahedral angle of rotation, α, used to define the position of the rigid SiO_4 tetrahedra was defined by them as the smaller of the two angles between the O-O tetrahedral edge normal to the $\bar{4}$ axis and the two orthogonal crystallographic axes that are perpendicular to it (Fig. 5). This angle, α, increases with decreasing size of the X-site cation (Born and Zemann 1964; Novak and Gibbs 1971; Meagher 1980; Armbruster and Geiger 1992). A plot of the tetrahedral angle of rotation against the radius of the X-site cation for synthetic end-member garnets pyrope, almandine, spessartine, and grossular is shown in Figure 6. The relationship is nonlinear. Using the geometrical constraints imposed by the high symmetry of the garnet structure (i.e., $Ia\bar{3}d$), Born and Zemann (1964) were able to relate the unit-cell dimension, a_0, and the tetrahedral angle of rotation, under the assumption of rigid tetrahedra and constant Al-O bond lengths in garnet. They derived the following equations:

$$x = R \cdot a_o^{-1} \cdot \cos \varphi \quad (4)$$

$$y = R \cdot a_o^{-1} \cdot \sin \varphi \cdot \sin \alpha \quad (5)$$

$$z = R \cdot a_o^{-1} \cdot \sin \varphi \cdot \cos \alpha \quad (6)$$

where x, y, and z are the atomic fractional coordinates of the O atoms, R is the Si-O distance, φ is an internal tetrahedral angle (see Born and Zemann 1964), and α is the tetrahedral angle of rotation. The question is whether the measured molar volumes of mixing of the different garnet solid solution binaries relate to structural changes that can be described by the amount of tetrahedral rotation.

It is observed in the aluminosilicate garnets that the two binaries pyrope-grossular (Wood 1988; Ganguly et al. 1993; Bosenick and Geiger, unpublished manuscript) and almandine-grossular (Cressey et al. 1978; Geiger et al. 1987; Koziol 1990) display the largest positive deviations from ideal mixing. The ΔV^{mix} curves are asymmetric, meaning that at low grossular contents they are

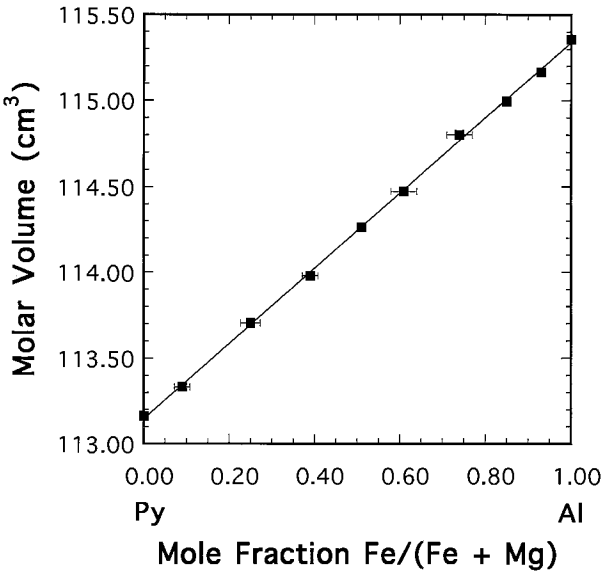

FIGURE 3. Molar volumes for the solid solution pyrope-almandine. The solid line is a linear least-squares fit to the data. The error bars represent one standard deviation in the compositions as determined from microprobe analyses. The uncertainties in the molar volumes are smaller than the size of the symbols.

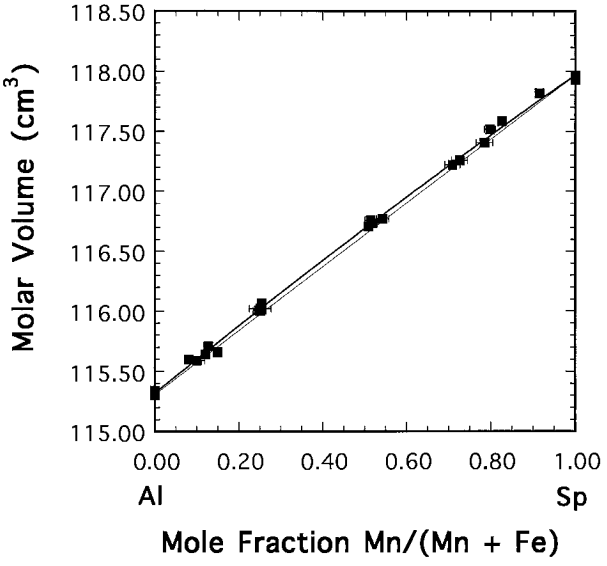

FIGURE 4. Molar volumes for the solid solution almandine-spessartine. The upper solid curve gives a least-squares quadratic polynomial fit to the data. The thin line defines ideal mixing between almandine and spessartine. The error bars represent one standard deviation in the compositions as determined from microprobe analyses. The uncertainties in the molar volumes are smaller than the size of the symbols.

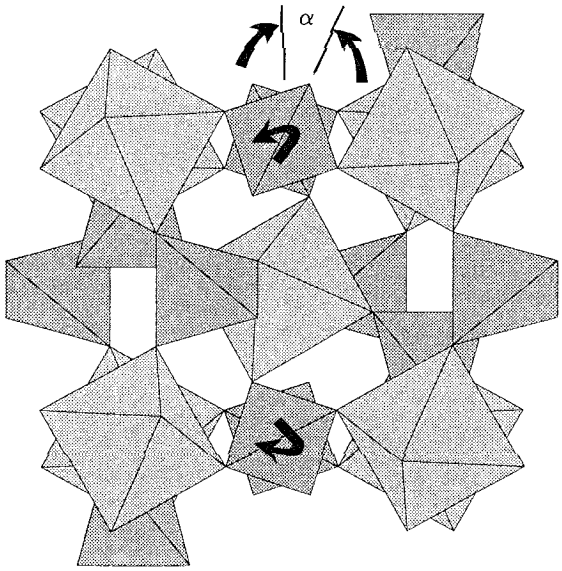

FIGURE 5. Polyhedral model of the garnet structure viewed down the *c* axis. The corner-linked, rigid tetrahedra and octahedra form a three-dimensional framework. The divalent cations (not shown) occupy the large cavities and are surrounded by eight O atoms in dodecahedral coordination. The arrows in the tetrahedra show rotations to smaller values of α.

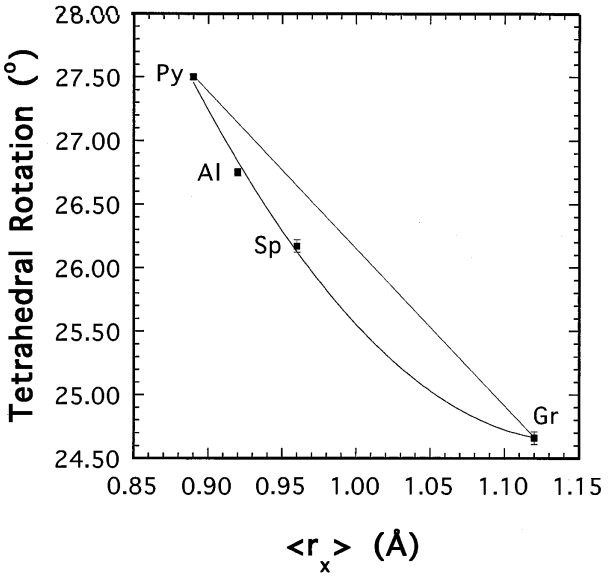

FIGURE 6. Plot of the tetrahedral rotation angle, α, vs. the radius of the X-site cation for synthetic end-member aluminosilicate garnets. The straight line connects pyrope and grossular, and the curved line is a quadratic fit to the data and has no physical significance. The data are from Armbruster et al. (1992) for pyrope, Geiger et al. (1992) for almandine, and Geiger and Armbruster (1997) for spessartine and grossular. The ionic radii are from Shannon (1976).

relatively ideal and at higher grossular contents the strongest positive deviations from ideal mixing occur. Figure 7 shows the tetrahedral angle of rotation, α, along the pyrope-grossular binary, calculated using the O atom coordinates determined in a powder X-ray Rietveld study (Ganguly et al. 1993). It shows that the tetrahedral angle of rotation along the solid-solution join also displays an asymmetric trend analogous to the volumes of mixing. The substitution of relatively small amounts of the large cation Ca (i.e., <20 mol% grossular) into the pyrope structure can be described by a linear change in the tetrahedral angle of rotation between pyrope and grossular. However, with increasing grossular contents the angle of rotation deviates from this simple linear relationship. It appears that deviations from ideal volumes of mixing along this join relate to the degree of tetrahedral rotation. High-precision single-crystal X-ray diffraction data are needed to test this proposal critically. We believe the calculated averaged tetrahedral rotations of Py-Gr solid solutions are not greatly influenced by local site deformations, inasmuch as the four aluminosilicate end-members show a similar relationship (Fig. 6).

Based on five single-crystal X-ray refinements, the Al-Py binary displays an essentially linear change in the tetrahedral angle of rotation going from end-member pyrope to almandine (Armbruster et al. 1992). Here, the difference between the ionic radii of Fe^{2+} (0.92 Å; Shannon 1976) and Mg (0.89 Å) is smaller than between (Mg,Fe^{2+}) and Ca (1.10 Å) in the Py-Gr and Al-Gr binaries. Koziol (1990) proposed that the volumes of mixing of Sp-Gr garnets can be described as ideal. Following

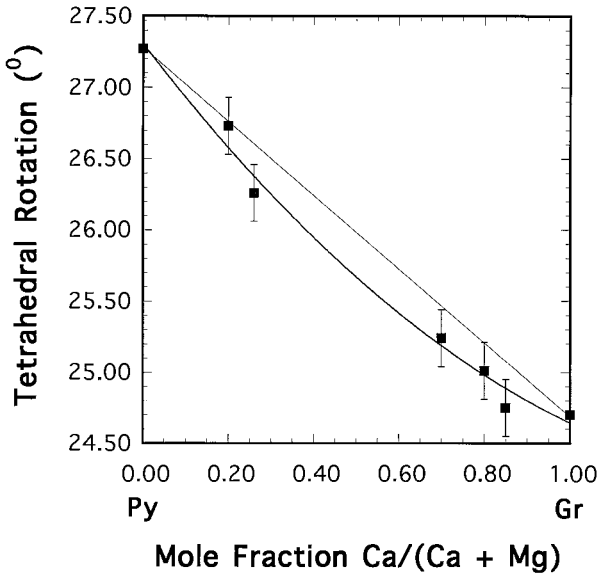

FIGURE 7. Plot of the tetrahedral rotation angle, α, along the join pyrope-grossular. The Rietveld data of Ganguly et al. (1993) were used to calculate α. The straight line connects pyrope and grossular, and the curved line is a quadratic fit to the data. The error bars give the uncertainties resulting from the errors in the coordinates of the O atom.

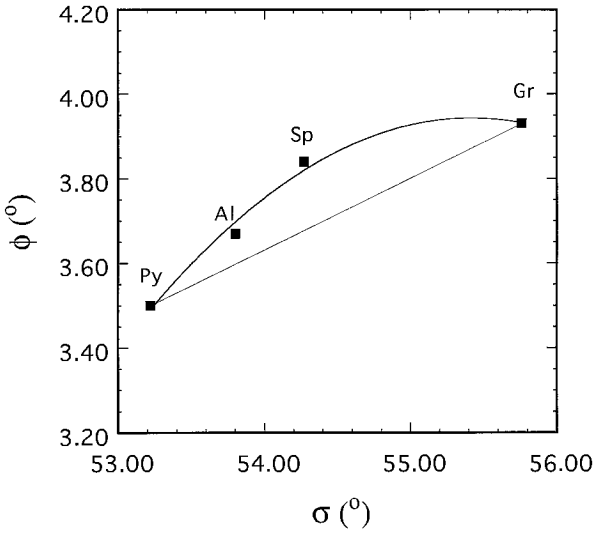

FIGURE 8. Plot of dodecahedral distortion (ϕ) vs. octahedral-tetrahedral distortion (σ) for the aluminosilicate garnets. The straight line connects pyrope with grossular, and the curved line is a quadratic fit to the data. The sources of the data are the same as those used in Figure 6.

this analysis, this join should be expected to show positive deviations from ideality and, hence, additional careful unit-cell refinements are required to test this interpretation.

Limits to the extent of cation substitution in the X site, with respect to the maximum size of the X-site cation, should be counterbalanced by the nature of the edge-sharing arrangement between dodecahedra and tetrahedra-octahedra (see Born and Zemann 1964 for a more complete discussion). The large number of shared polyhedral edges acts to buttress and stiffen the framework and should limit the degree of tetrahedral rotation. Figure 8 shows a plot of the two functions, ϕ and σ (Euler and Bruce 1965), which can be used to describe dodecahedral bond-angle strain and octahedral-tetrahedral bond-angle strain, respectively (Novak and Gibbs 1971). The degree of dodecahedral distortion mimics and follows from the degree of tetrahedral rotation for the aluminosilicate garnets (Fig. 6).

Ungaretti et al. (1995) thoroughly analyzed the volumes of mixing of the aluminosilicate garnets using the results of 281 single-crystal X-ray refinements of garnets. They placed an emphasis on the distortion of the three different polyhedra in controlling the volumes of mixing. Moreover, they considered the bonding character of the X-site cations between the calcic and noncalcic garnets to be different and partly responsible for the crystal-chemical properties of both compositional types (with respect to the bonding character of Fe^{2+} in synthetic Al-Gr, Al-Py, and Al-Sp solid solutions, no difference could be detected considering the nearly compositionally independent isomer shifts recorded along all three solid solution binaries using Mössbauer spectroscopy (Geiger, unpublished data). The volumes of mixing calculated with their crystal-chemical model give positive symmetric deviations for the pyrope-grossular join and asymmetric volumes of mixing for the almandine-pyrope binary. On the other hand, our crystal-chemical interpretation places an emphasis on the tetrahedral angle of rotation in controlling the volumes of mixing. Although the other factors may play a role, we consider them to be secondary in importance. The amount of distortion of the dodecahedron and the bonding character of the X-site cation should follow from the degree of tetrahedral rotation. The degree of dodecahedral distortion and the bonding characteristics of the X-site cations are important for interpreting the vibrational entropies of mixing.

Volumes and entropies of mixing

Because volume and entropy are generally correlated thermodynamically, volumes of mixing are potentially useful in estimating vibrational entropies of mixing, the latter of which are laborious to determine experimentally. The thermodynamic relation between the two is given by:

$$\left(\frac{\partial S}{\partial V}\right)_T = \frac{\alpha}{\beta} = \left(\frac{\partial P}{\partial T}\right)_V. \quad (7)$$

Wood (1988) suggested that the excess vibrational entropies of mixing along the Py-Gr join are asymmetric in a sense similar to ΔV^{ex}. Thermal expansions are partly known for Py-Gr garnets (Bosenick and Geiger, unpublished manuscript), but the compressibilities for the solid solutions have not been measured. Positive asymmetric excess vibrational entropies of mixing along the garnet binaries Al-Gr and Py-Gr can be rationalized crystal-chemically by considering the vibrational behavior of the smaller of the two cations mixing in the dodecahedral site, Fe^{2+} and Mg, respectively, for Al-Gr and Py-Gr. With increasing substitution of the larger cation Ca in both solid solutions, the difference between the two independent X-O bond lengths increases and hence so does dodecahedral site distortion. Greater dodecahedral site distortion should allow the smaller of the two mixing cations to increase its freedom and amplitude of vibration in a larger and more distorted site (see Armbruster and Geiger 1993; Geiger and Armbruster 1997). This should occur in a nonlinear fashion following the degree of tetrahedral rotation (Fig. 7). Increased amplitudes and lower frequencies of vibration of the smaller X-site cation, relative to the almandine or pyrope end-members, may be a source of excess heat capacities in binaries where the volumes of mixing show positive deviations from ideality. In this static-based crystal-chemical model it can be expected that the Py-Gr and Al-Gr binaries would have the largest ΔS^{ex} and the Al-Py and Al-Sp joins the smallest ΔS^{ex}.

However, it must be stated that this analysis has ignored any potential complications related to localized dodecahedral distortions that may be of a different nature than those derived from diffraction experiments. They

must be accounted for spectroscopically (Geiger and Rossman 1994).

Moreover, dynamic aspects must also be considered. The masses of the mixing X-site cations must be accounted for in an analysis of the bonding and dynamical properties. It is the phonon density of states that governs the heat capacity (and vibrational entropy) of a substance. In the case of garnet, they have not been determined by inelastic neutron scattering measurements. They can be estimated, though, through measurements of the IR and Raman active modes and appropriate lattice dynamic models. A consideration of the IR active modes for Py-Gr garnets shows that the excess heat capacities of mixing at low temperatures (10–150 K; Haselton and Westrum 1980) and the ideal mixing behavior observed between 298 and 1000 K are consistent with the frequencies of the IR modes, because the lowest frequency modes of the solid solution compositions decrease in energy away from the end-members pyrope and grossular (Bosenick et al. 1996). These modes contribute heavily to the heat capacities at low temperatures.

Powder IR measurements on synthetic almandine-spessartine and almandine-pyrope solid solutions (Geiger, unpublished data) indicate a different behavior that shows the former binary should have no excess heat capacity of mixing at low temperatures. The Al-Py join, where the difference in mass between Fe^{2+} and Mg^{2+} is great, has a more complicated mode behavior at low energies, and hence small excess vibrational entropies of mixing may exist along this join. This analysis of the vibrational entropies of mixing is contrary to nearly all predictions in the mineralogical literature, which generally only consider the size of the mixing cations (i.e., static model) and hence predict ideal thermodynamic mixing for the pyrope-almandine join (Kravchuk 1981; Ganguly and Saxena 1984).

In conclusion, crystal-chemical data and the vibrational spectra of garnet yield important information on the bulk macroscopic thermodynamic mixing properties. ΔS^{mix} and ΔV^{mix} are, at least in the case of the aluminosilicate garnets, partly complementary and internally consistent. Well-determined molar volume of mixing data now exist for five of the binaries within the four-component garnet system almandine-pyrope-grossular-spessartine. Unit-cell measurements of pyrope-spessartine garnets are now required for a more complete description of the volume of mixing behavior in compositionally complex aluminosilicate garnets.

Acknowledgments

G.A. Lager and B.C. Chakoumakos undertook the Rietveld analyses and gave a critical reading of the manuscript. Uta Rodehorst measured the unit-cell dimensions of several garnets. H.St.C. O'Neill suggested that we look at the procedures adopted for fitting the volumes of mixing in an earlier version of this manuscript. J. Schimmler has been most generous in explaining the statistics of least-squares methods and in writing the computer programs for the different models. We thank them all. The work of C.A.G. has been supported by the Deutsche Forschungsgemeinschaft through grant Ge 649/2-2 as part of a priority program and that of A.F. by the Schweizerischer Nationalfonds. The latter grant also supported the Cameca SX-50 electron microprobe at the University of Bern (Grant 21-26579.89).

References cited

Anovitz, L.M., Essene, E.J., Metz, G.W., Bohlen, S.R., Westrum Jr, E.F., and Hemingway, B.S. (1993) Heat capacity and phase equilibria of almandine, $Fe_3Al_2Si_3O_{12}$. Geochemica et Cosmochimica Acta, 57, 4191–4204.

Armbruster, T., Geiger, C.A., and Lager, G.A. (1992) Single-crystal X-ray structure study of synthetic pyrope almandine garnets at 100 and 293 K. American Mineralogist, 77, 512–521.

Armbruster, T. and Geiger, C.A. (1993) Andradite crystal chemistry, dynamic X-site disorder and structural strain in silicate garnets. European Journal of Mineralogy, 5, 59–71.

Berkson, J. (1950) Are there two regressions? Journal of the American Statistical Association, 45, 164–180.

Bohlen, S.R., Wall, V.J., and Boettcher, A.L. (1983) Experimental investigations and geologic applications of equilibria in the system FeO-TiO_2-AI_2O_3-SiO_2-H_2O. American Mineralogist, 68, 1049–1058.

Born, L. and Zemann, J. (1964) Abstandsberechnungen und Gitterenergitische Berechnungen an Granate. Contributions to Mineralogy and Petrology, 10, 2–23.

Bosenick, A., Geiger, C.A., and Cemic, L. (1996) Heat capacity measurements of synthetic pyrope-grossular garnets between 320 and 1000 K by Differential Scanning Calorimetry. Submitted to Geochimica et Cosmochimica Acta, 60, 3215–3227.

Cressey, G., Schmid, R., and Wood, B.J. (1978) Thermodynamic properties of almandine-grossular garnet solid solution. Contributions to Mineralogy and Petrology, 67, 397–404.

Deming, W.E. (1964) Statistical Adjustment of Data. Dover, New York.

Euler, F. and Bruce, J.A. (1965) Oxygen coordinates of compounds with garnet structure. Acta Crystallographica, 19, 971–978.

Ganguly, J. and Saxena, S.K. (1984) Mixing properties of aluminosilicate garnets: constraints from natural and experimental data, and applications to geothermo-barometry. American Mineralogist, 69, 88–97.

Ganguly, J., Cheng, W., and O'Neill, H.St.C. (1993) Syntheses, volume, and structural changes of garnets in the pyrope-grossular join: Implications for stability and mixing properties. American Mineralogist, 78, 583–593.

Geiger, C.A. (1993) ^{57}Fe-Mössbauer spectroscopy of almandine-spessartine garnets. Eos, 74, 676.

Geiger, C.A. and Armbruster, T. (1997) $Mn_3Al_2Si_3O_{12}$–spessartine and $Ca_3Al_2Si_3O_{12}$–grossular garnet: Structural dynamic and thermodynamic properties. American Mineralogist, in press.

Geiger, C.A., Newton, R.C., and Kleppa, O.J. (1987) Enthalpy of mixing of synthetic almandine-grossular and almandine-pyrope garnets from high temperature solution calorimetry. Geochimica et Cosmochimica Acta, 51, 1755–1763.

Geiger, C.A., Langer, K., Winkler, B., and Cemic, L. (1988) The synthesis, characterization and physical properties of end-member garnets in the system (Fe, Mg, Ca, Mn)$_3$Al$_2$(SiO$_4$)$_3$. In H. Vollstadt, Ed., High pressure geosciences and material synthesis, p. 193–198. Adademie-Verlag, Berlin.

Geiger, C.A., Langer, K., and Winkler, B. (1989) Infrared spectra of synthetic almandine-grossular and almandine-pyrope garnet solid solutions: Evidence for equivalent site behavior. Mineralogical Magazine, 53, 231–237.

Geiger, C.A., Lottermoser, W., and Amthauer, G. (1990) A temperature dependent ^{57}Fe Mössbauer study of synthetic almandine-grossular and almandine-pyrope garnets: A comparison. Third International Symposium of Experimental Mineralogy, Petrology and Geochemistry, p. 11. Edinburgh, U.K.

Geiger, C.A., Langer, K., Bell, D.R., Rossman, G.R., and Winkler, B. (1991) The hydroxide component in synthetic pyrope. American Mineralogist, 76, 49–59.

Geiger, C.A., Armbruster, T., Jiang, K., Lager, G.A., Lottermoser, W., and Amthauer, G. (1992) A combined temperature dependent ^{57}Fe Mössbauer and single crystal X-ray diffraction study of synthetic almandine: Evidence for the Goldanskii-Karyagin effect. Physics and Chemistry of Minerals, 19, 121–126.

Geiger, C.A. and Rossman, G.R. (1994) Crystal field stabilization energies

of almandine-pyrope and almandine-spessartine garnets determined by FTIR near infrared measurements. Physics and Chemistry of Minerals, 21, 516–525.

Haselton, H.T. and Westrum, E.F., Jr. (1980) Low-temperature heat capacities of synthetic pyrope, grossular and pyrope*60*geossular*40*. Geochimica et Cosmochimica Acta, 44, 701–709.

Hill, R.J. (1985) Refinement of the structure of orthorhombic PbO (Massicot) by Rietveld analysis of neutron powder diffraction data. Acta Crystallography, C41, 1281–1284.

Hsu, L.C. (1968) Selected phase relations in the system Al-Mn-Fe-Si-O-H: A model for garnet equilibria. Journal of Petrology, 9, 40–83.

Hummel, W. (1988) GITTER, Version 2.0. Berechnung von Gitterparametern aus Röntgen-Pulverdiagrammen. Laboratorium für Chemische und Mineralogische Kristallographie, Universität Bern.

Koziol, A.M. (1990) Activity-composition relationships of binary Ca-Fe and Ca-Mn garnets determined by reversed, displaced equilibrium experiments. American Mineralogist, 75, 319–327.

Kravchuk, I.V. (1981) Energy relations, thermodynamics, and stability of solid solutions of garnets. Geochemistry International, 18, no.1, 73–79 (translated from Geokhimiya, no. 1, 121–128, 1981).

Menzer, G. (1928) Die Kristallstruktur der Granate. Zeitschrift für Kristallographie, 69, 300–396.

Merli, M., Callegari, A., Cannillo, E., Caucia, F., Leona, M., Oberti, R., and Ungaretti, L. (1995) Crystal-chemical complexity in natural garnets: structural constraints on chemical variability. European Journal of Mineralogy, 7, 1239–1249.

Meagher, E.P. (1980) Silicate Garnets. In Mineralogical Society of America Reviews in Mineralogy, 5, 301–367.

Mottana, A. (1974) Melting of spessartine at high pressure. Neues Jahrbuch für Mineralogie, Monatshefte, 256–271.

Novak, G.A. and Gibbs, G.V. (1971) The crystal chemistry of the silicate garnets. American Mineralogist, 56, 791–825.

Shannon, R.D. (1976) Revised effective ionic radii and systematic studies of interatomic distances in halides and chalcogenides. Acta Crystallographica, A32, 751–767.

Thompson, J.B., Jr. (1967) Thermodynamic properties of simple solutions. In P.H. Abelson, Ed., Researches in Geochemistry, vol. 2, p. 340–361. Wiley, New York.

Ungaretti, L., Leona, M., Merli, M., and Oberti, R., (1995) Non-ideal solid-solution in garnet: crystal-structure evidence and modelling. European Journal of Mineralogy, 7, 1299–1312.

Wiles, D.B. and Young, R.A. (1981) A new computer program for Rietveld analysis of X-ray powder diffraction patterns. Journal of Applied Crystallography, 14, 149–151.

Wood, B.J. (1988) Activity measurements and excess entropy-volume relationships for pyrope-grossular garnets. Journal of Geology, 96, 721–729.

Zemann, J. (1962) Zur Kristallchemie der Granate. Beiträge zur Mineralogie und Petrographie, 8, 180–188.

Manuscript received March 1, 1995
Manuscript accepted February 10, 1997